CHAPTER 19

Mechanical Response of Cytoskeletal Networks

Margaret L. Gardel,[*] Karen E. Kasza,[†] Clifford P. Brangwynne,[†] Jiayu Liu,[‡] and David A. Weitz[†,‡]

[*]Department of Physics and Institute for Biophysical Dynamics
University of Chicago, Illinois 60637

[†]School of Engineering and Applied Sciences
Harvard University
Cambridge, Massachusetts 02143

[‡]Department of Physics
Harvard University
Cambridge, Massachusetts 02143

METHODS IN CELL BIOLOGY, VOL. 89

0091-679X/08 $35.00
DOI: 10.1016/S0091-679X(08)00619-5

Abstract

The cellular cytoskeleton is a dynamic network of filamentous proteins, consisting of filamentous actin (F-actin), microtubules, and intermediate filaments. However, these networks are not simple linear, elastic solids; they can exhibit highly nonlinear elasticity and athermal dynamics driven by ATP-dependent processes. To build quantitative mechanical models describing complex cellular behaviors, it is necessary to understand the underlying physical principles that regulate force transmission and dynamics within these networks. In this chapter, we review our current understanding of the physics of networks of cytoskeletal proteins formed *in vitro*. We introduce rheology, the technique used to measure mechanical response. We discuss our current understanding of the mechanical response of F-actin networks, and how the biophysical properties of F-actin and actin cross-linking proteins can dramatically impact the network mechanical response. We discuss how incorporating dynamic and rigid microtubules into F-actin networks can affect the contours of growing microtubules and composite network rigidity. Finally, we discuss the mechanical behaviors of intermediate filaments.

I. Introduction

Many aspects of cellular physiology rely on the ability to control mechanical forces across the cell. For example, cells must be able to maintain their shape when subjected to external shear stresses, such as forces exerted by blood flow in the vasculature. During cell migration and division, forces generated within the cell are required to drive morphogenic changes with extremely high spatial and temporal precision. Moreover, adherent cells also generate force on their surrounding environment; cellular force generation is required in remodeling of extracellular matrix and tissue morphogenesis.

This varied mechanical behavior of cells is determined, to a large degree, by networks of filamentous proteins called the cytoskeleton. Although we have the tools to identify the proteins in these cytoskeletal networks and study their structure and their biochemical and biophysical properties, we still lack an understanding of the biophysical properties of dynamic, multiprotein assemblies. This knowledge of the biophysical properties of assemblies of cytoskeletal proteins is necessary to link our knowledge of single molecules to whole cell physiology. However, a complete understanding of the mechanical behavior of the dynamic cytoskeleton is far from complete.

One approach is to develop techniques to measure mechanical properties of the cytoskeleton in living cells (Bicek *et al.*, 2007; Brangwynne *et al.*, 2007a; Crocker and Hoffman, 2007; Kasza *et al.*, 2007; Panorchan *et al.*, 2007; Radmacher, 2007). Such techniques will be critical in delineating the role of cytoskeletal elasticity in dynamic cellular processes. However, because of the complexity of the living cytoskeleton, it would be impossible to elucidate the physical origins of this cytoskeletal elasticity from live cell measurements in isolation. Thus, a complementary

approach is to study the behaviors of reconstituted networks of cytoskeletal proteins *in vitro*. These measurements enable precise control over network parameters, which is critical to develop predictive physical models. Mechanical measurements of reconstituted cytoskeletal networks have revealed a rich and varied mechanical response and have required the development of qualitatively new experimental tools and physical models to describe physical behaviors of these protein networks. In this chapter, we review our current understanding of the biophysical properties of networks of cytoskeletal proteins formed *in vitro*. In Section II, we discuss rheology measurements and the importance of several parameters in interpretation of these results. In Section III, we discuss the rheology of F-actin networks, highlighting how small changes in network composition can qualitatively change the mechanical response. In Section IV, the effects of incorporating dynamic microtubules in composite F-actin networks will be discussed. Finally, in Section V, we will discuss the mechanics of intermediate filament (IF) networks.

II. Rheology

Rheology is the study of how materials deform and flow in response to externally applied force. In a simple elastic solid, such as a rubber band, applied forces are stored in material deformation, or strain. The constant of proportionality between the stress, force per unit area, and the strain, deformation per unit length, is called the elastic modulus. The geometry of the measurement defines the area and length scale used to determine stress and strain. Several different kinds of elastic moduli can be defined according to the direction of the applied force (Fig. 1). The tensile

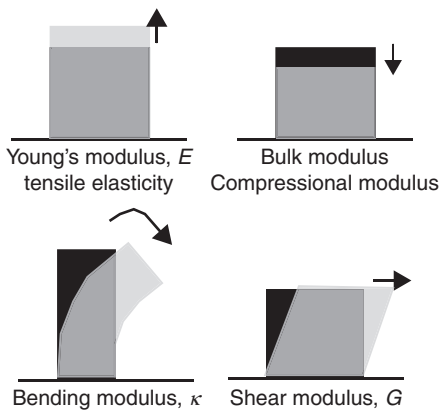

Fig. 1 Schematics showing the direction of the applied stress in several common measurements of mechanical properties; the light gray shape, indicating the sample after deformation, is overlaid onto the black shape, indicating the sample before deformation. The Young's modulus, or tensile elasticity, is the deformation in response to an applied tension whereas the bulk (compressional) modulus measures material response to compression. The bending modulus measures resistance to bending of a rod along its length and, finally, the shear modulus measures the response of a material to a shear deformation.

elasticity, or Young's modulus, is determined by the measurement of extension of a material under tension along a given axis. In contrast, the bulk modulus is a measure of the deformation under a certain compression. The bending modulus of a slender rod measures the object resistance to bending along its length. And, finally, the shear elastic modulus describes object deformation resulting from a shear, volume-preserving stress (Fig. 2). For a simple elastic solid, a steady shear

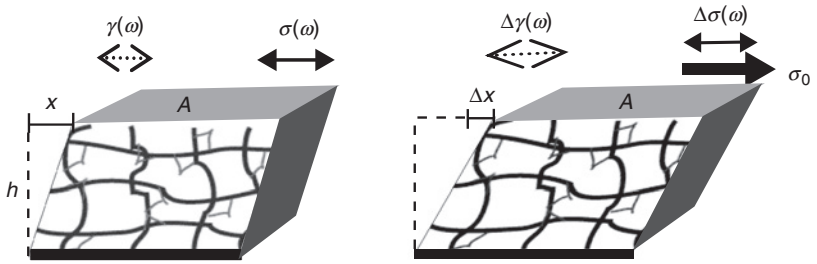

Term	Symbol	Units	Definition
Strain	γ	None	$\frac{x}{Height\ (h)}$; sample deformation
Stress	σ	Pascal (Pa)	$\frac{Force}{Area\ (A)}$
Frequency	ω	Time^{-1}	Frequency of applied + measured waveforms: $\gamma(\omega) = \gamma \sin(\omega t)$, $\sigma(\omega) = \sigma \sin(\omega t)$
Prestress	σ_0	Pascal (Pa)	Constant external stress applied to sample during measurement
Phase Shift	δ	Degrees	$\delta(\omega) = \tan^{-1}(G''(\omega)/G'(\omega))$ $\delta = 0°$, elastic solid; $\delta = 90°$, fluid
Shear moduli:			
$\sigma_0 = 0$			
Elastic (storage) modulus	G'	Pascal (Pa)	$G'(\omega) = \sigma(\omega)/\gamma(\omega) \cos(\delta(\omega))$
Viscous (loss) modulus	G''	Pascal (Pa)	$G''(\omega) = \sigma(\omega)/\gamma(\omega) \sin(\delta(\omega))$
$\sigma_0 > 0$			
Differential elastic modulus	K'	Pascal (Pa)	$K'(\omega) = \Delta\sigma(\omega)/\Delta\gamma(\omega) \cos(\Delta\delta(\omega))$
Differential loss modulus	K''	Pascal (Pa)	$K'(\omega) = \Delta\sigma(\omega)/\Delta\gamma(\omega) \cos(\Delta\delta(\omega))$

Fig. 2 This schematic defines many of the rheology terms used in this chapter. (Left) To measure the shear elastic modulus, $G'(\omega)$, and shear viscous modulus, $G''(\omega)$, an oscillatory shear stress, $\sigma(\omega)$, is applied to the material and the resultant oscillatory strain, $\gamma(\omega)$ is measured. The frequency, ω, is varied to probe mechanical response over a range of timescales. (Right) To measure how the stiffness varies as a function of external stress, a constant stress, σ_0, is applied and a small oscillatory stress, ($\Delta\sigma(\omega)$), is superposed to measure a differential elastic and viscous loss modulus.

stress results in a constant strain. In contrast, for a simple fluid, such as water, shear forces result in a constant flow or rate of change of strain. The constant of proportionality between the stress and strain rate, $\dot{\gamma}$, is called the viscosity, η.

To date, most rheological measurements of cytoskeletal networks have been that of the shear elastic and viscous modulus. Mechanical measurements of shear elastic and viscous response over a range of frequencies and strain amplitudes are possible with commercially available rheometers. Recent developments in rheometer technology now provide the capability of mechanical measurements with as little as 100 μl sample volume, a tenfold decrease in sample volume from previous generation instruments. Recently developed microrheological techniques now also provide measurement of compressional modulus (Chaudhuri *et al.*, 2007). Reviews of microrheological techniques can be found in Crocker and Hoffman (2007), Kasza *et al.* (2007), Panorchan *et al.* (2007), Radmacher (2007), and Weihs *et al.* (2006).

A. Frequency-Dependent Viscoelasticity

In general, the rheological behaviors of cytoskeletal polymer networks display characteristics of both elastic solids and viscous fluids and, thus, are viscoelastic. To characterize the linear viscoelastic response, small amplitude, oscillatory shear strain, $\gamma \sin(\omega t)$, is applied and the resultant oscillatory stress, $\sigma \sin(\omega t+\delta)$, is measured , where δ is the phase shift of the measured stress and is $0 < \delta < \pi/2$. (Figure 2 describes much of the terminology used in this chapter.) The in-phase component of the stress response determines the shear elastic modulus, $G'(\omega) = (\sigma/\gamma)\cos(\delta(\omega))$, and is a measure of how mechanical energy is stored in the material. The out-of-phase response measures the viscous loss modulus, $G''(\omega) = (\sigma/\gamma)\sin(\delta(\omega))$, and is a measure of how mechanical energy is dissipated in the material. In general, G' and G'' are frequency-dependent measurements. Thus, materials that behave solid-like at certain frequencies may behave liquid-like at different frequencies; measurements of the frequency-dependent moduli of solutions of flexible polymers (polyethylene oxide) and the biopolymer, filamentous actin (F-actin) are shown in Fig. 3A. The solution of flexible polymers (black symbols) is predominately viscous, and the viscous modulus (open symbols) dominates over the elastic modulus (filled symbols) over the entire frequency range. In contrast, the solution of F-actin filaments (gray symbols, Fig. 3A) is dominated by the viscous modulus at frequencies higher than 0.1 Hz but becomes dominated by the elastic modulus at lower frequencies. Thus, it is critical to make measurements over an extended frequency range to ascertain critical relaxation times in the sample. Moreover, frequency-dependent dynamics should be carefully considered in establishing mechanical models.

The measurements shown in Fig. 3A are measurements of *linear* elastic and viscous moduli. In the linear regime, the stress and the strain are linearly dependent and, since the moduli are the ratio between these quantities, the measured moduli are independent of the magnitude of applied stress or strain. For flexible polymers, the moduli can remain linear up to extremely high (>100%) strains. (Consider

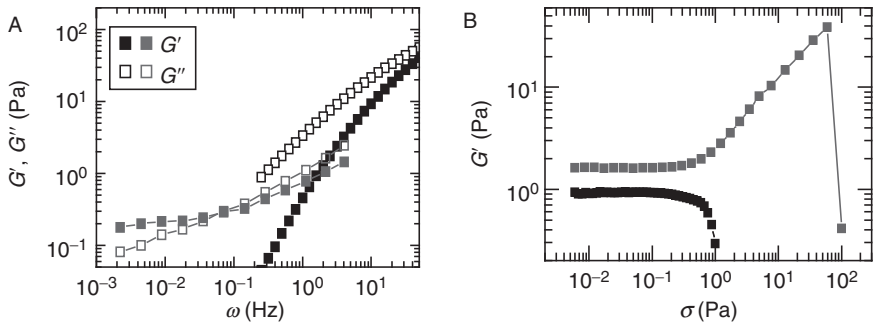

Fig. 3 (A) Frequency-dependent elastic (filled symbols) and viscous (open symbols) moduli of a network of F-actin (gray symbols) and solution of flexible polymers (black symbols) illustrating the frequency dependence of these parameters (B) Measurement of G' as a function of applied stress for a network that stress stiffens (top, gray squares) and stress weakens (bottom, black squares).

extending a rubber band; the force required to extend it a certain distance will remain linear up to several times its original length.) However, for many biopolymer networks, the linear elastic regime can be quite small (<10%). To confirm you are measuring linear elastic properties, it is recommended that you make measurements at two different levels of stress and confirm you measure identical frequency-dependent behaviors.

B. Stress-Dependent Elasticity

The mechanical response of cytoskeletal networks can be highly nonlinear such that the elastic properties are critically dependent on the stress that is applied to the network. When the elasticity increases with increasing applied stress or strain, materials are said to ''stress-stiffen'' or ''strain-stiffen'' (Fig. 3B). In contrast, if the elasticity decreases with increased stress, the material is said to ''stress-soften'' or, likewise, ''strain-soften'' (Fig. 3B).

Stress-stiffening behavior has been observed for many cytoskeletal networks, for example, F-actin networks cross-linked with a variety of actin-binding proteins (Gardel *et al.*, 2004a, 2006b; MacKintosh *et al.*, 1995; Storm *et al.*, 2005; Xu *et al.*, 2000) and intermediate filament networks (Storm *et al.*, 2005). In this nonlinear regime, F-actin networks compress in the direction normal to that of the shear and exert negative normal stress (Janmey *et al.*, 2007). The origins of stress-stiffening can occur in nonlinearities in elasticity of individual actin filaments or reorganization of the network under applied stress.

Not all reconstituted cytoskeletal networks exhibit stress stiffening under shear. Some show stress weakening: the modulus decreases as the applied stress increases. This is usually found in networks that are weakly connected. For example, pure F-actin solutions, weakly cross-linked actin networks (Gardel *et al.*, 2004a; Xu

et al., 1998), and pure microtubule networks (Lin *et al.*, 2007) all show stress-softening behavior. Under compression, branched, dendritic networks of F-actin are also shown to reversibly stress soften at high loads (Chaudhuri *et al.*, 2007).

In the nonlinear elastic regime, large amplitude oscillatory measurements are inaccurate, as the response waveforms are not sinusoidal (Xu *et al.*, 2000). To accurately measure the frequency-dependent nonlinear mechanical response, a static prestress can be applied to the network, and the linear, differential elastic modulus, K', and loss modulus, K'' are determined from the response to a small, superposed oscillatory stress (Gardel *et al.*, 2004a,b; Fig. 2, right). However, if a material remodels and the strain changes with time when imposed by a constant external stress alternative, nonoscillatory rheology measurements may be necessary.

C. Effect of Measurement Length Scale

Due to the inherent rigidity of cytoskeletal polymers, cytoskeletal networks formed *in vitro* are structured at micrometer length scales. The mechanical response of cytoskeletal networks can depend on the length scale at which the measurement is taken (Gardel *et al.*, 2003; Liu *et al.*, 2006). Conventional rheometers measure average mechanical response of a material at length scales $>100\ \mu$m. By contrast, microrheological techniques can be used to measure mechanical response at micrometer length scales; however, interpretations of these measurements are not usually straightforward for cytoskeletal networks structured at micrometer length scales (Gardel *et al.*, 2003; Valentine *et al.*, 2004; Wong *et al.*, 2004). Direct visualization of the deformations of filaments such as F-actin and microtubules (Bicek *et al.*, 2007; Brangwynne *et al.*, 2007a) can also be used to calculate local stresses (see Section IV).

III. Cross-Linked F-Actin Networks

A. Biophysical Properties of F-Actin and Actin Cross-linking Proteins

1. Actin Filaments

Actin is the most abundant protein found in eukaryotic cells. It comprises 10% of the total protein mass in muscle cells and up to 5% in nonmuscle cells (Lodish *et al.*, 1999). Globular actin (G-actin) polymerizes to form F-actin with a diameter, d, of 5 nm and contour lengths, L_c, up to 20 μm (Fig. 4). The extensional modulus, or Young's modulus, E, of F-actin is approximately 10^9 Pa, similar to that of plexiglass (Kojima *et al.*, 1994). However, due to the nanometer-scale filament diameter, the bending modulus, $\kappa_0 \sim Ed^4$, is quite soft. The ratio of κ_0 to thermal energy, k_BT, defines a length scale called the persistence length, $\ell_p \sim \kappa_0/k_BT$. This is the length over which vectors tangent to the filament contour become uncorrelated by the effects of thermally driven bending fluctuations. For F-actin, $\ell_p \approx 8 - 17\mu$m, (Gittes *et al.*,

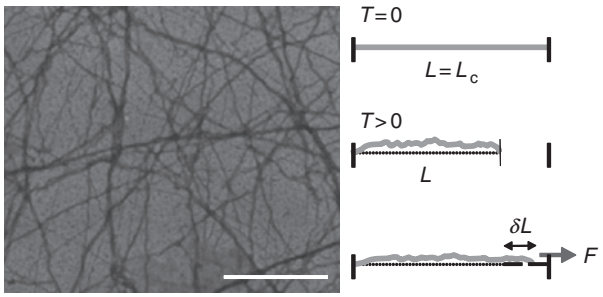

Fig. 4 (Left) Electron micrograph of F-actin. Scale bar is 1 μm. (Right) In the absence of thermal forces ($T = 0$), a semiflexible polymer appears as a rod, with the full polymer contour length, L_c, identical to the shortest distance between the ends of the polymer, L. However, thermally induced transverse bending fluctuations ($T > 0$) lead to contraction of L such that $L < L_c$. An applied tensile force, F, extends the filament by a length, δL, and, because L_c is constant, this reduces the amplitude of the thermally induced bending fluctuations, giving rise to a force-extension relation that is entropic in origin.

1993; Ott *et al.*, 1993) and, thus, is semiflexible at micrometer length scales with a persistence length intermediate to that of DNA, $\ell_p \approx 0.05$ μm, and microtubules, $\ell_p \approx 1000$ μm.

Transverse fluctuations driven by thermal energy ($T > 0$) also result in contraction of the end-to-end length of the polymer, L, such that $L < L_c$ (Fig. 4). In the linear regime, applied tensile force, τ, to the end of the filament results in extension, δL, of the filament such that: $\tau \sim [\kappa^2/(\kappa T L^4)] \times (\delta L)$ (MacKintosh *et al.*, 1995). This constant of proportionality, $\kappa^2/(\kappa T L^4)$, defines a spring constant that arises from purely thermal effects, which seek to maximize entropy by maximizing the number of available configurations of the polymer. The distribution and number of available configurations depends on the length, L, of the polymer such that the spring constant will decrease simply by increasing filament length. However, as $L \to L_c$, the entropic spring constant diverges such that the force-extension relationship is highly nonlinear (Bustamante *et al.*, 1994; Fixman and Kovac, 1973; Liu and Pollack, 2002). At high extension, the tensile force diverges nonlinearly with increasing extension such that: $\tau \sim 1/(L_c - L)^2$. Thus, the force-extension relationship depends sensitively on the magnitude of extension.

The elastic properties of actin filaments are also sensitive to binding proteins and molecules. For instance phalloidin and jasplakinolide, two small molecules that stabilize F-actin enhance F-actin stiffness (Isambert *et al.*, 1995; Visegrady *et al.*, 2004). It has been shown that a member of the formin family of actin-binding and nucleator proteins, mDia1, decreases the stiffness of actin filaments (Bugyi *et al.*, 2006).

2. Actin Cross-Linking Proteins

In the cytoskeleton, the local microstructure and connectivity of F-actin is controlled by actin-binding proteins (Kreis and Vale, 1999). These binding proteins control the organization of F-actin into mesh-like gels, branched dendritic

networks, or parallel bundles, and it is these large-scale cytoskeletal structures that determine force transmission at the cellular level. Some proteins, such as fimbrin and α-actinin, are small and tend to organize actin filaments into bundles, whereas others, like filamin and spectrin, tend to organize F-actin into more network-like structures.

The cross-linking proteins found inside most cells are quite different from simple rigid, permanent cross-links in two important ways. Most physiological cross-links are dynamic, with finite binding affinities to actin filaments that results in the disassociation of cross-links from F-actin over timescales relevant for cellular remodeling. Moreover, physiological cross-links have a compliance that depends on their detailed molecular structure and determines network mechanical response. Thus, not surprisingly, the kinetics and mechanics of F-actin-binding proteins can have a significant impact on the mechanical response of cytoskeletal networks.

Typical F-actin cross-linking proteins are dynamic; they have characteristic on and off rates that are on the order of seconds to tens of seconds. The cross-linking protein α-actinin, which is commonly found in contractile F-actin bundles, is a dumb-bell shaped dimer with F-actin-binding domains spaced approximately 30 nm apart. Typical dissociation constants for α-actinin are on the order of $K_d = 1\ \mu M$ and dissociation rates are on the order of $1\ s^{-1}$, but vary between different isoforms (Wachsstock *et al.*, 1993), with temperature (Tempel *et al.*, 1996) and the mechanical force exerted on the cross-link (Lieleg and Bausch, 2007).

Physiologically relevant cross-links cannot be thought of simply as completely rigid structural elements; they can, in fact, contribute significantly to network compliance. Filamin proteins found in humans are quite large dimers of two 280-kDa polypeptide chains, each consisting of 1 actin-binding domain, 24 β-sheet repeats forming 2 rod domains, and 2 unstructured "hinge" sequences (Stossel *et al.*, 2001). The contour length of the dimer is approximately 150 nm, making it one of the larger actin cross-links in the cell (Fig. 5A). Unlike many other

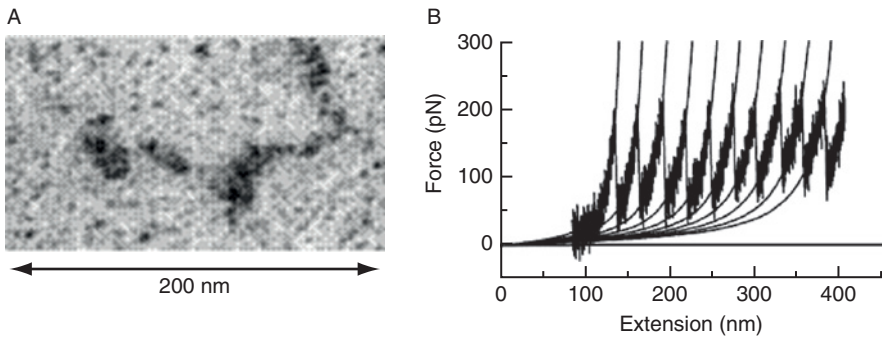

Fig. 5 (A) Electron micrographs of filamin A dimer (with permission, Stossel *et al.*, 2001). (B) Force-extension curve for a filamin A molecule measured by atomic force microscopy. The characteristic sawtooth pattern is associated with unfolding events of β-sheet domains in the molecule (with permission, Furuike *et al.*, 2001).

cross-linking proteins that dimerize parallel to each other in order to form a small rod, the filamin molecules dimerize such that they form a V-shape with actin-binding domains at the end of each arm. This geometry is thought to allow filamin molecules to preferentially cross-link actin filaments orthogonally and to form strong networks even at low concentrations.

The compliance of a single filamin molecule can be probed with atomic force microscopy force-extension measurements. Initial results suggest that for forces less than 50–100 pN, a single filamin A molecule can be modeled as a worm-like chain; for larger forces, reversible unfolding of β-sheet repeats occurs, leading to a large increase in cross-link contour length (Furuike *et al.*, 2001; Fig. 5B). It is important to note that forces reported for these types of unfolding measurements are rate dependent; the longer a force is applied to the molecule, the lower the threshold force required for the conformational change.

One additional class of binding proteins is molecular motors such as myosin. The conformation change of the molecule as it undergoes ATP hydrolysis can generate pico-Newton scale forces within the F-actin network or bundle. These forces can generate filament motion, such as observed in F-actin sliding within the contraction of a sarcomere. These actively generated forces can significantly change the mechanical properties and the structure of the cytoskeletal network in which they are embedded (Bendix *et al.*, 2008).

B. Rheology of Rigidly Cross-Linked F-Actin Networks

Although the importance of understanding mechanical response of cytoskeletal networks has been appreciated for several decades, predictive physical models to describe the full range of mechanical response observed in these networks have proven elusive. This has been, in part, due to the large sample volumes required by conventional rheology (1–2 ml per measurement) and the inability to purify sufficient quantities of protein with adequate purity to perform *in vitro* measurements. Improvement in the torque sensitivity of commercially available rheometers as well as the establishment of bacteria and insect cell expression systems for protein expression has overcome many of these difficulties.

In the last several years, much progress has been made in understanding the elastic response of F-actin filaments cross-linked into networks by very rigid, nondynamic linkers. This class of cross-linkers greatly simplifies the interpretations of the rheology in two distinct ways. When the cross-linkers are more rigid than F-actin filaments, then the mechanical response of the composite network is predominately determined by deformations of the softer F-actin filaments; in this case, the cross-linkers serve to determine the architecture of the network. When cross-linkers have a very high binding affinity and remain bound to F-actin over long times (>minutes), then we do not have to consider the additional timescales associated with cross-linking binding affinity, which can lead to network remodeling under external stress.

Two realizations of this are cross-linking through avidin–biotin cross-links (MacKintosh *et al.*, 1995) and the actin-binding protein, scruin (Gardel *et al.*, 2004a; Shin *et al.*, 2004). In these networks, network compliance is due to the semiflexibility of individual F-actin filaments. Such a network can be considered to have an average distance between actin filaments, or mesh size, $\xi \sim 1/\sqrt{c_A}$ with a distance between cross-links, ℓ_c where $\ell_c > \xi$ for homogeneous networks.

1. Network Elasticity and Microscopic Deformation

In order to establish an understanding of the elastic properties of a material, it is required to know how it will deform in response to an external shear stress. For semiflexible polymers, such as F-actin, strain energy can be stored either in filament bending or in stretching. These elastic constants depend on the length of filament segment that is being deformed, for instance, ℓ_c for a homogeneous cross-linked F-actin network. Recent theoretical work has shown that the deformation of F-actin networks under an external shear stress is dominated by stretching of filaments in the limit of high cross-link and F-actin concentration and long filament lengths (Head *et al.*, 2003a,b). Here, the deformations in the network are self-similar at all length scales, or affine (Fig. 6). In contrast, in the limit of low cross-link and F-actin concentration and short F-actin lengths, deformations imposed by the external shear stress result in filament bending and nonaffine deformation throughout the network (Das *et al.*, 2007;

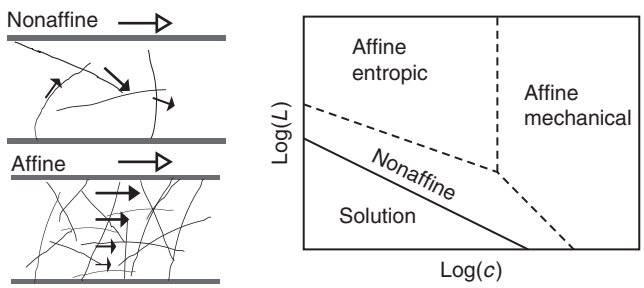

Fig. 6 (Left) Schematics indicating difference between affine and nonaffine deformations. A fibrous network is indicated by slender black rods that is confined between two parallel plates indicated by dark gray rods. The direction of shear at the macroscopic level is indicated by the arrow with the open arrowhead, whereas filled arrows indicate direction of microscopic deformations within the sample. In nonaffine deformations, the directions of deformation within the sample are not similar to each other or to the direction of macroscopic shear; this type of deformation is realized in very sparse networks. In affine deformation, the direction of macroscopic deformation is highly self-similar to the directions of microscopic deformation within the sample; this type of deformation is realized in highly concentrated polymer networks. (Right) A sketch of the various elastic regimes in terms of molecular weight L and polymer concentration c. The solid line represents where network rigidity first appears at the macroscopic level. For affine deformation, elastic response can arise both from the filament stretching of entropically derived bending fluctuations or from the Young's modulus of individual filaments.

Head *et al.*, 2003a,b; Fig. 6). These predictions have been confirmed in experiments by visualizing the deformations of F-actin networks during application of shear deformation using confocal microscopy (Liu *et al.*, 2007) where nonaffinity is calculated as the deviation of network deformations after shear from the assumed affine positions; these experiments confirmed that weakly cross-linked F-actin networks exhibited nonaffine deformations, whereas deformations of strongly cross-linked networks were more affine.

2. Entropic Elasticity of F–Actin Networks

In networks of F-actin cross-linked with incompliant cross-links where shear stress results in affine deformations, the elastic response is dominated by stretching of individual actin filaments. At the filament length scale, the strain, γ, is proportional to δ/ℓ_c where δ is the extension of individual filaments and ℓ_c is the distance between cross-links. The stress, σ, can be considered as F/ξ^2, where F is the force applied to individual filaments and ξ is the mesh size of the network. Thus, we can relate the force-extension of single filaments (Section III.A.1) to the network elasticity. For networks structured at micrometer length scales, the spring constant determined by entropic fluctuations determines the elastic response at small strains such that:

$$G' \sim \frac{\sigma}{\gamma} \sim \frac{\kappa^2}{k_B T \xi^2 \ell_c^3}$$

where the contour length is determined by the distance between cross-links and is proportional to the entanglement length. Because the entropic spring constant is highly sensitive to the contour length, this model predicts a sharp dependence of the elastic stiffness with both the F-actin concentration, c_A, and the ratio of cross-links to actin monomers, R, such that:

$$G' \sim c_A^{11/5} R^{(6x+15y)/5}$$

where the exponent x characterizes how efficiently the cross-linker bundles F-actin and y characterizes the cross-linking efficiency (Shin *et al.*, 2004). The variation of the elastic stiffness as a function of F-actin concentration has been observed experimentally (Gardel *et al.*, 2004a; MacKintosh *et al.*, 1995; Fig. 7). The pronounced dependence of the elastic stiffness observed as a function of polymer and cross-link density is in sharp contrast to the weak dependence observed in networks of flexible polymers.

Densely cross-linked F-actin networks exhibit nonlinear elasticity at large stresses and strains, where G' increases as a function of stress until a maximum stress,σ_{max}, and strain, γ_{max}, at which the network "breaks" (Fig. 2B). In this system, the breaking stress is linearly proportional to the density of F-actin filaments and suggests that individual F-actin ruptures (Gardel *et al.*, 2004b). The maximum strain is observed to vary such that $\gamma_{max} \sim \ell_c \sim c_A^{-2/5}$ and directly

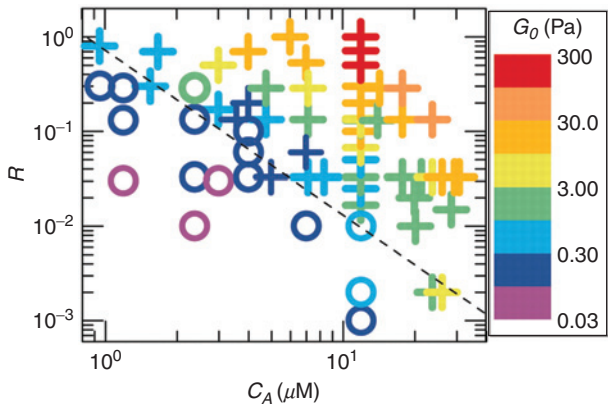

Fig. 7 State diagram of rigidly cross-linked F-actin networks over a range of R, the cross-link concentration, and c_A, F-actin concentration. The range in colors corresponds to the magnitude of the linear elastic modulus, G_0 (indicated by the heat scale) whereas the symbols denote networks that exhibit stress stiffening (+) or stress weakening (o) (with permission, Gardel *et al.*, 2004).

reflects the change in contour length resulting from varying F-actin concentration (Gardel *et al.*, 2004a). Moreover, the qualitative form of the nonlinearity in the stress–strain relationship at the network length scale is identical to divergence observed in the force–extension relationship for single semiflexible polymers as the extension approaches the polymer contour length (Gardel *et al.*, 2004a,b). Thus, the nonlinear strain-stiffening response of these F-actin networks at macroscopic length scales directly reflects the nonlinear stiffening of individual filaments.

3. Other Regimes of Elastic Response

As the concentration of cross-links or the filament persistence length increases, the entropic spring constant to stretch semiflexible filaments will increase sufficiently such that the deformation of filaments is dominated by the Young's modulus of the filament. Here, the elasticity is still due to stretching individual F-actin filaments, but thermal effects do not play a role and the elastic response of these networks is more similar to that of a dense network of macroscopic rods (e.g., imagine a dense network of cross-linked pencils or spaghetti). Here, no mechanism for significant stress stiffening at the scale of individual rods is established. However, reorganization of these networks under applied stress may lead to stress stiffening. Such a regime of elasticity may be observed in networks of highly bundled F-actin filaments; such networks have not been observed experimentally.

In contrast, as the density of cross-links or filament persistence length decreases, filaments will tend to bend (and buckle) under an external shear deformation. Bending deformations result in deformations that are not self-similar, or affine, within the network (Head *et al.*, 2003a,b). Experimental measurements have shown an increase

in nonaffine deformations at low cross-link concentrations (Liu *et al.*, 2007) as well as an abrogation of stress-stiffening response (Gardel *et al.*, 2004a). Instead, these networks soften under increasing strain and linear response is observed for strains as large as one. For these networks, the linear elastic modulus is less sensitive to variations in cross-link density and actin concentration. While a complete comparison with theory is still required, it appears that in this regime, network elasticity is dominated by filament bending, with nonlinear response due to buckling of single filaments (Gardel *et al.*, 2004a; Head *et al.*, 2003a,b; Liu *et al.*, 2007).

The rich variety of elastic response in even a model system of F-actin cross-linked by rigid, nondynamic cross-links demonstrates the complexity involved with building mechanical models of networks of cross-linked semiflexible polymers that can exhibit both entropic and enthalpic contributions to the mechanical response.

C. Physiologically Cross-Linked F-Actin Networks

F-actin networks formed with rigid, incompliant cross-links form a benchmark to understanding the elastic response of cytoskeletal F-actin networks. However, as discussed in Section III.A.2, physiological F-actin cross-linking proteins typically have a finite binding affinity to F-actin and significant compliance. The extent of F-actin-binding affinity of the cross-linker determines a timescale over which forces are efficiently transmitted through the F-actin/cross-link connection and dramatically affects how forces are transmitted and dissipated through the network. When the cross-link that has comparable stiffness to that of an F-actin filament, the network will elasticity will some superposition of the elastic response of each element individually. Thus, the changes in the kinetics and mechanics of individual cross-linking proteins can dramatically affect the mechanical response of the F-actin network.

1. Effects of Cross-Link Binding Kinetics: α-Actinin

The contribution of cross-link binding kinetics to network material properties has been studied most explicitly in the α-actinin and fascin systems. The dynamic nature of cytoskeletal cross-links means that networks formed with them are able to reorganize and remodel, or look ''fluid-like'' at long times (Sato *et al.*, 1987). In particular, temperature has been used to systematically alter the binding affinity of α-actinin to F-actin, and the mechanics of the resulting network probed with bulk rheology (Tempel *et al.*, 1996; Xu *et al.*, 1998). The key experimental observation is that as temperature is increased from 8 to 25 °C, the α-actinin cross-linked F-actin networks become softer and more fluid-like. At 8 °C, the networks are stiff, elastic networks that look similar to networks cross-linked with rigid, static cross-links. As the temperature is raised to 25 °C, the network stiffness decreases by nearly a factor of 10 and the network becomes more fluid-like.

There are a variety of effects that could contribute to this behavior, including changes to F-actin dynamics and the fraction of bound α-actinin cross-links. However, these experiments found that the dominant effect of increasing

temperature is to increase the rate of α-actinin unbinding from F-actin, implying that as cross-link dissociation rates increase, the network becomes a more dynamic structure that can relax stress. This suggests that if cells require cytoskeletal structures to reorganize and remodel, it is important to have dynamic cross-link proteins like α-actinin, not permanent ones like scruin. One interesting example where cross-link binding kinetics has a strong biological consequence is in an α-actinin-4 isoform having a point mutation that causes increased actin-binding affinity (Weins *et al.*, 2005; Yao *et al.*, 2004). This increased binding affinity is associated with cytoskeletal abnormalities in focal segmental glomerulosclerosis, a lesion found in kidney disease that results from a range of disorders including infection, diabetes, and hypertension.

Mechanical load can also have an effect on cross-link binding kinetics. When large shear stresses are applied to fascin cross-linked and bundled F-actin networks, network elasticity depends on the forced unbinding of cross-links in a manner that depends on the rate at which stress is applied (Lieleg and Bausch, 2007). Although temperature is unlikely to be an important control parameter *in vivo*, mechanical force on actin-binding proteins may regulate both mechanical response of the network and organization of signaling within the cytoplasm. However, it is unknown to what extent cross-link kinetics play a role in regulation of mechanical stresses within live cells to enable rapid and local cytoskeletal reorganization.

2. Effect of Cross-Link Compliance: Filamin A

Cross-link geometry and compliance can also contribute significantly to F-actin network elasticity. Rigidly cross-linked networks have a well-defined elastic plateau where the elastic modulus is orders of magnitude larger than the viscous modulus, and energy is stored elastically in the network. In contrast, networks formed from F-actin cross-linked with filamin A (FLNa) have an elastic modulus that is only two or three times the viscous modulus, and the elastic modulus decreases as a weak power law over timescales between a second and thousands of seconds (Gardel *et al.*, 2006a,b) (Fig. 8), similar to the timescale dependence of the elasticity of living cells (Fabry *et al.*, 2001). Moreover, in contrast to the F-actin–scruin networks where the linear elastic modulus can be tuned over several orders of magnitude by varying cross-link density, the linear elastic modulus for F-actin–FLNa networks is only weakly dependent on the FLNa concentration and is typically in the range of 0.1–1 Pa (Gardel *et al.*, 2006a), less than tenfold larger than for F-actin solutions formed without any cross-links.

Insight into how cross-link compliance can alter macroscopic mechanical response can be gained from a recent experiment in which the total length of the cross-link ddFLN, a filamin isoform from *Dictyostelium discoideum*, is systematically altered and the mechanics of the resulting network are probed using bulk rheology (Wagner *et al.*, 2006). In these networks, as the length of the cross-linker is systematically increased, the stress transmission in networks becomes

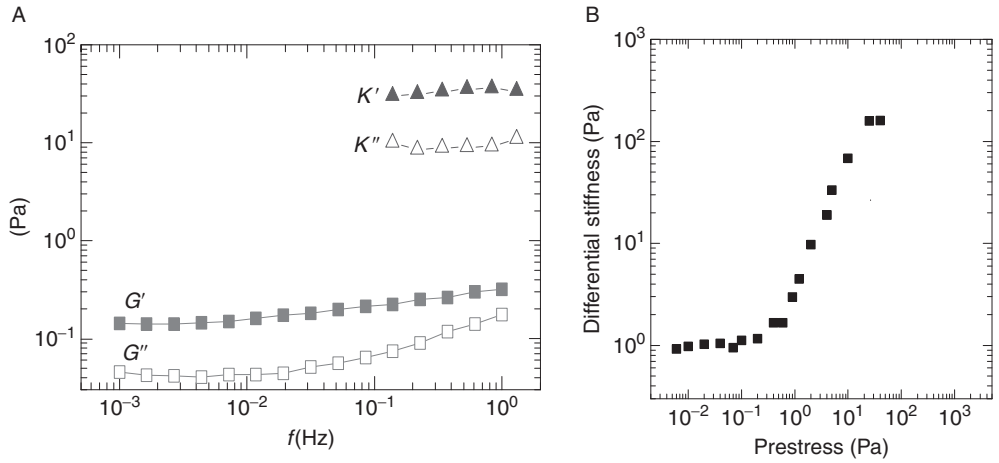

Fig. 8 (A) Frequency-dependent rheology of *in vitro* actin-filamin networks. In the linear regime, the network is a weak, viscoelastic solid with the elastic modulus, G' (closed gray squares), only a few time larger than the viscous modulus, G'' (open gray squares), over a broad range of frequencies. Upon application of a large steady shear stress ($\sigma_0 = 20$ Pa), the network stiffens dramatically; the differential shear moduli, K' (closed gray triangles) and K'' (open gray triangles), are two orders of magnitude larger than the linear moduli (with permission, Gardel *et al.*, 2006). (B) Differential shear elastic modulus of *in vitro* actin networks cross-linked with the physiologically relevant cross-linking protein filamin. Application of a prestress stiffens the networks by two orders of magnitude to the stiffness of typical living cells.

increasingly fluid-like: the magnitude of the elastic modulus decreases and becomes more sensitive to frequency.

Similar to rigidly cross-linked actin networks, FLNa cross-linked F-actin networks show strong nonlinear strain-stiffening behavior. At low stresses, the linear elastic modulus is approximately 1 Pa; at a critical stress of 0.5 Pa and critical strain of about 15%, the network can stiffen by over two orders of magnitude and support a maximum stress up to 100 Pa (Gardel *et al.*, 2006b). This remarkable nonlinear stiffening is a larger percentage over the linear elasticity than reported for any other cross-linked F-actin network. The network stiffness varies linearly as a function of applied stress to vary the differential stiffness from 1 Pa up to 1000 Pa (Fig. 8), stiffnesses that are characteristic of living cells. This system strongly suggests that nonlinear elastic effects may play an important role in determining the mechanical response of the cellular cytoskeleton.

Unlike in the F-actin–scruin system where network failure is consistent with F-actin filament rupture, the maximum stress that the F-actin–FLNa networks can withstand before breaking depends strongly on FLNa concentration, again highlighting the fact that FLNa contributes significantly to the overall network elasticity. The F-actin–FLNa networks allow very large strains, on the order of 100%, before network failure, whereas F-actin–scruin networks typically break at much smaller strains of around 30%. It is still unknown whether the F-actin–FLNa network

mechanical response arises merely from the large size, geometry, and compliance of the FLNa molecules or if, in fact, the stresses in the networks are large enough to unfold the β-sheet repeat sequences in the molecule so that the extensibility and flexibility of the FLNa molecule are further enhanced. In the ddFLN system, the maximum stress and strain supported by these networks increase with cross-link length (Wagner *et al.*, 2006), suggesting that the cross-link size itself is an important factor. Together, these results strongly suggest that the detailed microstructure of cross-linking proteins is critically important to the ability of the network to support large stresses and deformations without breaking.

Thus, it is not clear in networks of F-actin cross-linked with α-actinin or FLNa what the exact mechanism of network failure is. Actin filament rupture, cross-link rupture, F-actin-cross-link unbinding, and poor adhesion of the network to the site of applied force are all possibilities. Single-molecule experiments are starting to give good approximations for the rate-dependent breakage forces for both the F-actin and the cross-links (Furuike *et al.*, 2001). In all of these cases, the stress and strain at which the network fails can depend on the magnitude and duration of stress applied to the network and the details of how these stresses are felt by the individual network components at the microscopic scale. There is much interest in understanding the mechanical failure of cytoskeletal network for understanding biological phenomena ranging from cell shape and polarization to cell blebbing to symmetry breaking in model actin-based propulsion systems (Paluch *et al.*, 2006).

3. Effect of Myosin-II Motors

In the cellular cytoskeleton, F-actin is also cross-linked by minifilaments (8–13) of myosin-II motors to form contractile networks. In highly organized F-actin bundles, such as sarcomeres, conformational changes in the myosin-II motor proteins result in sliding of F-actin and shortening of bundle length. It has been observed that, at sufficiently high motor activity, the myosin–actin networks remain isotropic, but myosin-II-induced F-actin sliding accelerates mechanical relaxations within the network to fluidize the F-actin network (Humphrey *et al.*, 2002). However, as the percentage of active myosin-II motors decreases by ATP depletion, the tight, rigor binding of ADP-bound myosin-II to the F-actin serves to cross-link filaments. In this regime, the F-actin filaments *in vitro* condense into compact gels and self-organize into asters (Smith *et al.*, 2007). After full ATP depletion, these structures are stabilized and the elastic stiffness of these networks can be 100-fold enhanced over those F-actin solutions in the absence of myosin-II (Mizuno *et al.*, 2007). Moreover, the degree of stiffening observed in these networks is correlated to the concentration of active myosin-II; this suggests that nonlinear elastic stiffening due to motor proteins within the networks at the molecular scale is, to some degree, similar to that of external shear stresses imposed at the macroscopic level (Bendix *et al.*, 2008). These two competing roles of fluidization and stiffening of myosin-II at different levels of activity underscore the importance of the regulation of myosin-II activity in determining how forces

are transmitted through these networks in live cells. Further work is required to delineate the role of different cross-linking proteins and other mechanisms of myosin-II regulation in understanding force transmission through these contractile networks.

The nonlinear mechanics of *in vitro* cross-linked F-actin networks suggests a mechanism by which a cell can actively regulate its stiffness: embedded motor proteins apply stress to the actin cytoskeleton and push it into the nonlinear strain-stiffening regime. In this scheme, motor protein activity, not the exact concentration of cross-link, would set the local cell stiffness. This is consistent with known effects of internally generated myosin-II forces on cytoskeletal organization and mechanical response (Mizuno *et al.*, 2007). These behaviors suggest that the cellular cytoskeleton is composed of elements under tension, as described in tensegrity models (Ingber, 1997).

IV. Effects of Microtubules in Composite F-Actin Networks

In addition to F-actin, the cytoskeleton of eukaryotic cells is also composed of a network of microtubule filaments that plays a large number of important biological roles. Structurally, these filaments are hollow tubes and have remarkable features that are very different from those of F-actin. Within the composite cytoskeletal network, microtubules can give rise to complementary and, in some cases, synergistic mechanical properties. Microtubules are highly dynamic, exhibiting repeated cycles of growth and rapid depolymerization known as dynamic instability (Mitchison and Kirschner, 1984). This dynamic behavior allows microtubules to rapidly restructure into different functional network architectures; these include the highly specialized mitotic spindle within dividing cells, and the radial microtubule network that controls directional migration of polarized interphase cells. In addition to the capability for rapid restructuring, the microtubule network must also exhibit mechanical stability under load. For example, microtubules continually experience mechanical loads from motor proteins that drag their cargo through the cell along microtubule tracks. Actomyosin contractility is also known to mechanically load microtubules during cell migration (Waterman-Storer and Salmon, 1997) and during the periodic contractility of beating heart cells (Brangwynne *et al.*, 2006). Indeed, some models of cytoskeleton mechanics propose that the microtubule network functions as the compressive load-bearing component of the cytoskeleton, balancing tensile forces generated by actomyosin contractility (Ingber, 2003). Mechanical stability of the microtubule network is clearly necessary for its varied tasks within the cell.

Microtubules have a high bending rigidity that arises from their large diameter, $D \sim 25$ nm. The mechanical properties of the microtubule wall appear roughly similar to those of the actin backbone, $E \sim 1$ GPa, although the wall is not truly an isotropic continuum material, and its precise mechanical rigidity may depend on

the details of the applied stress (de Pablo *et al.*, 2003; Needleman *et al.*, 2004). However, as a first approximation, a continuum elastic picture holds remarkably well: since the bending rigidity scales as $\kappa \sim d^4$, microtubules should have a persistence length about $(25/7)^4 \sim 160$ times larger than actin filaments, in agreement with measurements showing $\ell_p^{MT} \sim 1$mm. Measurements of the mechanical properties of microtubules have been performed using a variety of techniques that actively apply a force and then determine the resulting bending, including optical tweezers (Felgner *et al.*, 1996; Kikumoto *et al.*, 2006), hydrodynamic flows (Kowalski and Williams, 1993; Venier *et al.*, 1994), osmotic pressure (Needleman *et al.*, 2004), and atomic force microscopy (de Pablo *et al.*, 2003). However, as with F-actin and other microscopic polymers, microtubules are subjected to randomly fluctuating thermal forces, and passive mechanical measurements utilizing these fluctuations are also frequently used for measuring microtubule bending rigidity (Brangwynne *et al.*, 2007a; Gittes *et al.*, 1993; Janson and Dogterom, 2004; Pampaloni *et al.*, 2006).

A. Thermal Fluctuation Approaches

Direct observation of conformational changes induced by thermal energy can be used as a powerful probe of the dynamic mechanical response of biopolymer filaments. The essential principle behind this technique arises from the equipartition theorem of statistical mechanics, whereby it can be shown that, on average, an independent (quadratic) mode of a system in thermal equilibrium has, on average, $k_B T$ of energy. Since the extent of bending that corresponds to this energy scale is determined by the rigidity of the filament, this rigidity can be determined by simply measuring the average magnitude of thermally induced bending fluctuations. The power of this simple idea can be fully exploited by tracing the entire contour of a freely fluctuating filament. At each time point, the contour is then subjected to Fourier analysis by decomposing its tangent angle as a function of arc length, $\theta(s)$, into a sum of cosine modes: $\theta(s) = \sqrt{2/L}\sum_{n=0}^{\infty} a_q \cos(qs)$ (Gittes *et al.*, 1993). Here, the Fourier amplitude, a_q, describes the amplitude of bending at wave vector, q, the inverse length scale over which bending takes place, $\lambda = 2\pi/q$, as shown schematically in Fig. 9. Bending fluctuations from one time to the next can be characterized by the mean-squared fluctuation in mode amplitude: $\langle \Delta a_q(\Delta t)^2 \rangle \equiv 1/2 \langle \left(a_q(t+\Delta t) - a_q(t) \right)^2 \rangle_\tau$, where Δt is the lag time. For thermally fluctuating filaments in aqueous buffer, the fluctuations are predicted to behave according to $\langle \Delta a_q(\Delta t)^2 \rangle \equiv (1 - e^{-\Delta t/\tau}) k_B T/\kappa q^2$ (Brangwynne *et al.*, 2007a; Gittes *et al.*, 1993), where τ is a relaxation time that determines the timescale over which successive shapes remain correlated. For $\Delta t \ll \tau$, the mode fluctuations grow linearly in time, whereas for $\Delta t \gg \tau$, the mode fluctuations will be saturated to the equilibrium values $\langle \Delta a_q^2 \rangle = k_B T/\kappa q^2$. Microtubules fluctuating in a quasi-2D chamber are well described by these equations, and one finds microtubule

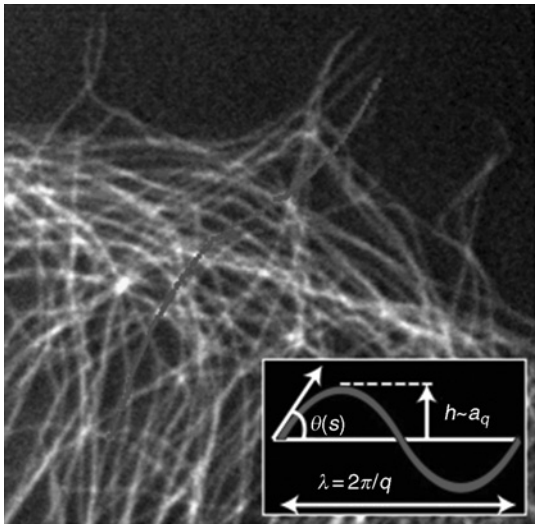

Fig. 9 Fluorescently labeled microtubules showing highly bent shapes, with a single microtubule highlighted. The inset defines the parameters used to extract the amplitude, a_q, and the wavelength, λ, of the Fourier modes describing the contour of the microtubule.

persistence lengths on the order of 1 mm. However, using such an approach, it has been suggested that a population of microtubules has heterogeneous bending behaviors that are more complex than that of actin filaments, arising from the fact that the wall of the tube is actually composed of an assembly of protofilaments (Brangwynne *et al.*, 2007a). Using a similar approach, it was shown that microtubules appear to have a bending rigidity that depends on their speed of polymerization (Janson and Dogterom, 2004). Moreover, another recent study suggests that the bending rigidities of microtubules may in fact depend on the length scale of the measurement (Pampaloni *et al.*, 2006); however, a similar finding was mistakenly reported for actin filaments (Kas *et al.*, 1993), and such behavior can arise from improper consideration of the experimental noise (Brangwynne *et al.*, 2007a). In addition to affecting the bending rigidity, the hierarchical microtubule structure may also contribute to an anomalous behavior of the bending timescales. Specifically, hydrodynamic drag is predicted to give rise to a relaxation time, $\tau \sim \eta/\kappa q^4$; actin filament fluctuations show good agreement with this predicted behavior (Brangwynne *et al.*, 2007a). In contrast, microtubules appear to exhibit a slight deviation from this hydrodynamic scaling at high wave vector (Janson and Dogterom, 2004), possibly due to the effects of internal dissipation mechanisms (Brangwynne *et al.*, 2007a; Poirier and Marko, 2002). These considerations suggest that the mechanical behavior of microtubules may actually be more variable and complex than previously believed; however, care must be taken in interpreting these experiments, since even in the absence of bending, the mode amplitudes will fluctuate due to noise (Brangwynne *et al.*, 2007a).

B. *In Vitro* MT Networks

There have been few studies of *in vitro* networks composed of purified microtubules. This is likely to change since the unique mechanical properties of these filaments will lead to interesting network properties different from those of actin filament networks. In particular, the mesh size of an *in vitro* microtubule network will be orders of magnitude smaller than the microtubule persistence length, and thus thermal fluctuations are likely to be negligible. This will give rise to very different behavior at high strain, as well as a high-frequency scaling unlike the $t^{3/4}$ scaling observed in actin networks (Koenderink *et al.*, 2006). Moreover, if the fluctuation timescales of microtubules are dominated by internal dissipation on short-length scales, the high-frequency rheological behaviors of microtubule networks may exhibit distinct and interesting scaling behaviors that have yet to be explored.

Microtubules in cells are typically embedded in the surrounding cytoskeletal network, and composite actin–microtubule networks are increasingly studied. A recent study focused on the fluctuation dynamics of individual filaments in a network of microtubules within an entangled actin network (Brangwynne *et al.*, 2007b). Because the network is not purely elastic, the Fourier spectrum of these fluctuating microtubules exhibits long-time saturating fluctuations that obey $\langle \Delta a_q^2 \rangle = k_B T/\kappa q^2$, with a corresponding persistence length approximately 1 mm, similar to the behavior of microtubules thermally fluctuating in aqueous buffer. Their relaxation dynamics are subdiffusive, reflecting fluctuations in a viscoelastic background medium; however, the long-time relaxation behavior is roughly consistent with the hydrodynamic prediction, $\tau \sim \eta_{\text{eff}}/\kappa q^4$, with an effective long-time viscosity, η_{eff}, about 1000 times that of water. If the actin network were cross-linked, behaving as a true elastic solid, the fluctuations of embedded microtubules would be restricted beyond a length scale, $\ell \sim (\kappa/G')^{1/4}$, where G' is the elastic modulus of the network; in this case, the saturating behavior $\langle \Delta a_q^2 \rangle = k_B T/\kappa q^2$ would not be observed.

This microscopic picture of the dynamics of microtubule fluctuations may begin to shed light on the bulk mechanical behavior of composite F-actin–microtubule networks. Recent work suggests that microtubules play a role in changing the internal deformation field of such networks in an important way. As described in Section III.B.1, at low cross-link density, an F-actin network will deform non-affinely under an applied stress, whereas at higher cross-link density, the network will transit into an affine entropic deformation regime associated with the important nonlinear strain-stiffening response. When microtubules are added to this network, this affine transition occurs at much lower cross-link density. The stiff microtubule rods appear to help homogenize the strain distribution in the actin network, and the local mechanical deformations reflect the bulk mechanical deformation, even at low cross-link density (Y.C. Lin, in preparation). This behavior suggests that the microtubule network could play an important role in controlling the nonlinear response of the prestressed cytoskeleton.

These findings also suggest that motor-driven composite F-actin–microtubule networks may be of particular interest. Indeed, microtubules may help facilitate the motor-induced nonlinear stiffening response of the network by ensuring that the deformation is locally affine. Moreover, it is conceivable that microtubules could help balance the internal prestress of "free-standing" cytoskeletal networks, enabling a nonlinear strain-stiffening response even in nonadherent cells or those only weakly coupled to the extracellular matrix (Ingber, 2003).

Although to our knowledge there are no published studies of the bulk mechanical response of motor-driven composite actin–microtubule networks, a recent study investigates the nonequilibrium dynamical behavior of microtubules in a composite network driven by myosin-II force generation (Brangwynne *et al.*, 2007b). Here, the bending dynamics of microtubules are used to determine the local force fluctuations within the network. In the absence of motors, a microtubule in an entangled actin network only undergoes small thermal fluctuations that evolve subdiffusively, as described above. However, in the presence of myosin motors, microtubules undergo large, highly localized bending fluctuations that exhibit rapid, step-like relaxation behavior. The localized bends are well-described by the function: $\gamma(x) = \gamma_0[\sin(|x|/\ell) + \cos(|x|/\ell)]e^{-|x|/\ell}$ that characterizes the bending of a rod embedded in an elastic material under the action of localized transverse forces. From the amplitude, γ_0, forces on the order of approximately 10 pN were determined, consistent with the action of a few myosin motors. As above, the decay length, $\ell \sim (\kappa/G')^{1/4}$, arises as a natural consequence of the competition between microtubule bending and deformation of the surrounding elastic network; the measured value, $\ell \sim 1 - 2$ μm, is consistent with the elastic modulus obtained from independent rheology measurements. Such localized fluctuations give rise to anomalously large Fourier bending amplitudes, particularly on short-length scales. Interestingly, the dynamics of these driven Fourier modes appear to be diffusive, consistent with step-like relaxations of force arising from binding and rapid unbinding of force-generating myosin. Because the microtubules are not cross-linked to the actin network, compressive forces cannot be maintained. Future work will focus on tuning the network interactions by cross-linking microtubules to the F-actin network, as well as using various F-actin cross-linking proteins to tune the properties of the F-actin network itself.

C. Mechanics of Microtubules in Cells

Upon considering the mechanical aspects of microtubule behavior in cells, the first thing one will notice is that the microtubule network in cells is typically highly bent (Fig. 9). This has been suggested as evidence that microtubules experience significant mechanical loads in cells. In particular, a long-held view maintains that microtubules function as compressive load-bearing elements within the cytoskeleton, and these bends reflect large compressive forces generated within cells (Ingber, 1997, 2003). However, this view is controversial, and others maintain that microtubules can only bear small compressive loads since they are so long. But, several

studies noted that microtubules often appear to compressively buckle into short-wavelength bends at the leading edge of cells, with wavelengths on the order of 3 μm; as seen in Fig. 11. At first glance, this is unexpected, since the lowest energy bends are those on the longest wavelengths (small curvature). Long-wavelength bending in response to compressive forces is known as Euler buckling, and can be readily observed if one compresses a flexible rod, such as a plastic ruler or a coffee stirrer, with length, L: upon reaching a critical force of order $f_{\text{compress}} \sim \kappa/L^2$, it will buckle into a single long arc. Isolated microtubules that are compressively loaded will undergo a similar buckling behavior, and the resulting shape can be quantitatively described by classic Euler buckling (Dogterom and Yurke, 1997).

While isolated microtubules buckle into long wavelengths, microtubules in cells are not isolated but rather are surrounded by other components of the composite cytoskeletal network. As described above for composite *in vitro* networks, the surrounding elastic network gives rise to a natural length scale of lowest-energy bending. As a result, microtubules will indeed buckle into short-wavelength shapes, with a wavelength given by $\lambda \sim (K/G)^{1/4}$. This physical behavior can be demonstrated in a simple model system consisting of a plastic rod embedded in elastic gelatin, as shown in Fig. 10. With appropriate prefactors, one can estimate that in cells, the buckling wavelength should be approximately 2 μm.

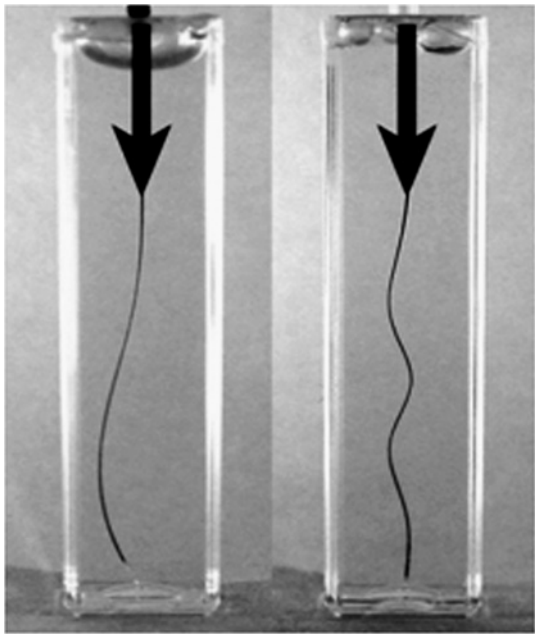

Fig. 10 The effect of compressive force on a plastic rod embedded in a purely viscous fluid (left) and a soft elastic gel, gelatin (right).

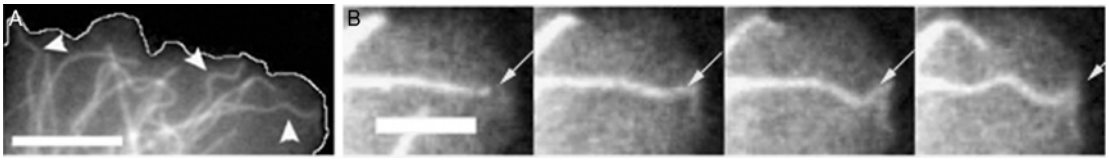

Fig. 11 (A) Fluorescently tagged microtubules in an adherent cell exhibit short-wavelength bends. Scale bar = 10 μm. (B) A magnified view of a microtubule from (A) buckling against the leading edge of the cell. Scale bar = 5 μm.

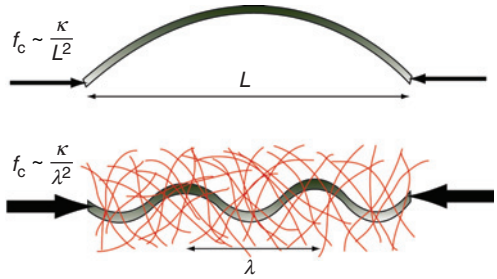

Fig. 12 Schematic showing the critical buckling force, f_c, in the absence (top) and presence (bottom) of a surrounding elastic matrix. In the presence of a surrounding elastic matrix, the characteristic bending wavelength is reduced, $\lambda < L$, such that f_c is substantially increased.

As described in a recent study, microtubules in cells indeed buckle on short wavelengths of approximately 3 μm in response to compressive loads generated by adherent epithelial cells, and in response to the periodic actomyosin contractility of beating heart cells (Brangwynne *et al.*, 2006). Moreover, initially straight microtubules can be made to buckle into this same short-wavelength shape by exogenous compressive forces applied with a microneedle. Unlike isolated rods undergoing simple Euler buckling, for this type of constrained short-wavelength buckling response, the critical buckling force is $f \sim \kappa/\lambda^2$. Microtubules in cells are typically tens of micrometers long. Thus, the buckling wavelength is on the order of ten times smaller than the total length, and the critical force is larger by a factor of approximately 100. This short-wavelength buckling response is thus indicative of a surrounding elastic network that effectively reinforces microtubules, allowing them to bear much larger compressive forces in cells, as shown schematically in Fig. 12.

In spite of the short-wavelength bending characteristic of composite microtubule networks, microtubules in cells also exhibit long-wavelength bends. The origin of this was addressed in a recent study, in which Fourier analysis of an ensemble of microtubule shapes in cells revealed bends on both short and long

wavelengths (Brangwynne *et al.*, 2007c). Moreover, this Fourier spectrum is remarkably thermal-like, with $\langle a_q^2 \rangle = (1/l_p^{\text{apparent}})(1/q^2)$. However, unlike microtubules in thermal equilibrium, the persistence length associated with this spectrum, l_p^{apparent}, is approximately 30 μm, about 100 times smaller than *in vitro* measurements. This is very surprising because even if some thermal-like agitation were the cause, there is no reason to expect a thermal-like spectrum, since, as discussed above, the surrounding network completely changes the energetics of microtubule bending.

By studying the time-dependent bending of individual microtubules, the bending fluctuations were found to be roughly diffusive, $\langle \Delta a_q(\Delta t)^2 \rangle \sim \Delta t$, similar to the behavior of thermally fluctuating microtubules in aqueous buffer. However, the cytoplasm is viscoelastic, and if thermal fluctuations were the cause, the bending fluctuations should be subdiffusive, as described above for microtubules thermally fluctuating in a composite actin–microtubule network. Moreover, these fluctuations are actually only significant on short-length scales. In contrast, the long-wavelength bends are effectively frozen-in; for an instantaneous bend with a wavelength of 10 μm, it would take approximately 1000 s to fully fluctuate to the ensemble-averaged values, which is longer than the lifetime of most microtubules (Schulze and Kirschner, 1986). Thus, unlike equilibrium materials, $\langle a_q^2 \rangle \neq \langle \Delta a_q^2 \rangle$, the cell exhibits behavior analogous to that of nonergodic materials far from thermal equilibrium. Indeed, while intracellular microtubule bending appears thermal-like, this behavior is actually completely analogous to microtubule dynamics in motor-driven composite actin networks (Brangwynne *et al.*, 2007b), suggesting that similar motor-driven, step-like stress relaxation dynamics also occur in cells.

This nonergodicity, or ''frozen-ness'', of long-wavelength microtubule bends suggests that microtubules may actually grow into these highly bent shapes. To test this, the trajectories of growing microtubule tips were tracked, using the microtubule tip-tracking protein Clip-170. This reveals that microtubules indeed grow into highly bent shapes; moreover, these trajectories exhibit a Fourier spectrum that closely resembles that of the ensemble spectrum of instantaneous shapes. This is consistent with a model in which the bending fluctuations of microtubules reorient the tips of growing microtubules, leading to a persistent random walk growth trajectory and a corresponding $\langle a_q^2 \rangle \sim 1/q^2$ mode spectrum; a simulation of this type of growth process, and the resulting thermal-like, but anomalously large Fourier spectrum, is shown in Fig. 13. Thus, the anomalous thermal-like instantaneous bending spectrum of intracellular microtubules appears to arise from the coupling of microtubule growth dynamics and non-thermal intracellular stress fluctuations within the composite cytoskeleton. The resulting small apparent persistence length, approximately 30 μm, has important implications for the ability of microtubules to rapidly restructure by dynamic instability, and their ability to stochastically locate cytoplasmic targets by the search and capture mechanism (Kirschner and Mitchison, 1986).

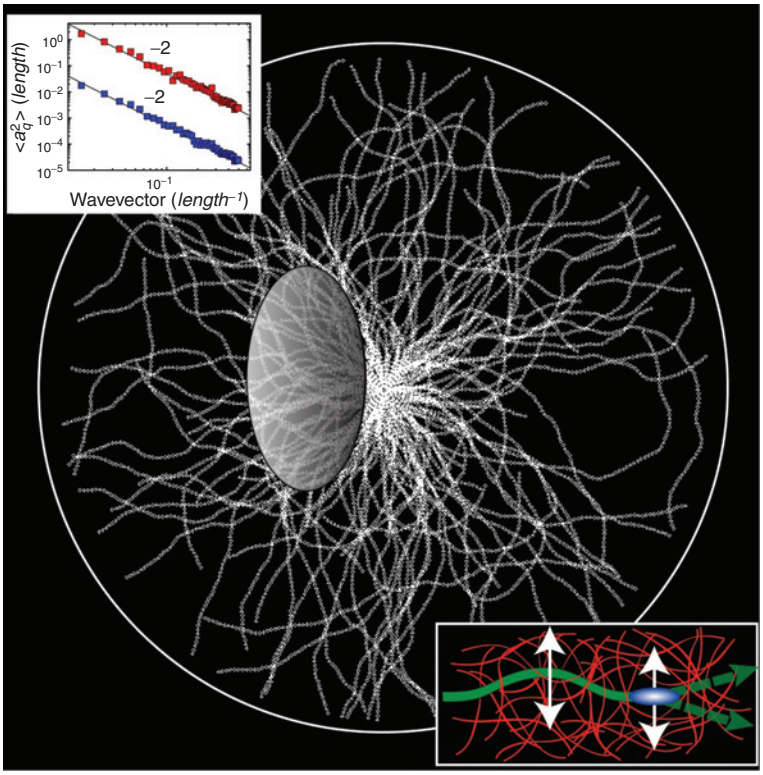

Fig. 13 Simulation to examine the contour of dynamic microtubules in the presence of nonthermal stress fluctuations. Top inset: The mode spectrum as a function of wave vector calculated for this simulation, using a small nonthermal (top) and large thermal (bottom) persistence length. Bottom inset: Schematic showing how lateral bending fluctuations will reorient the growing microtubule tip.

V. Intermediate Filament Networks

A. Introduction

A large family of proteins, collectively referred to as intermediate filaments (IFs), is the third and less well-studied class of biopolymers found in the cytoskeleton. Each IF protein, including keratins, vimentin, desmin, neurofilaments, and lamins, has a distinct chemical structure and function within the cell (Fig. 14). For example, vimentin localizes to the cytoplasm, often forms a composite network with both F-actin and microtubules, and is thought to be responsible for the cellular mechanical integrity. Lamins, on the other hand, maintain the shape and mechanical stability of the nucleus.

All IF proteins can assemble into approximately 10-nm-wide filaments. The particular architecture of IFs is important for understanding their unique

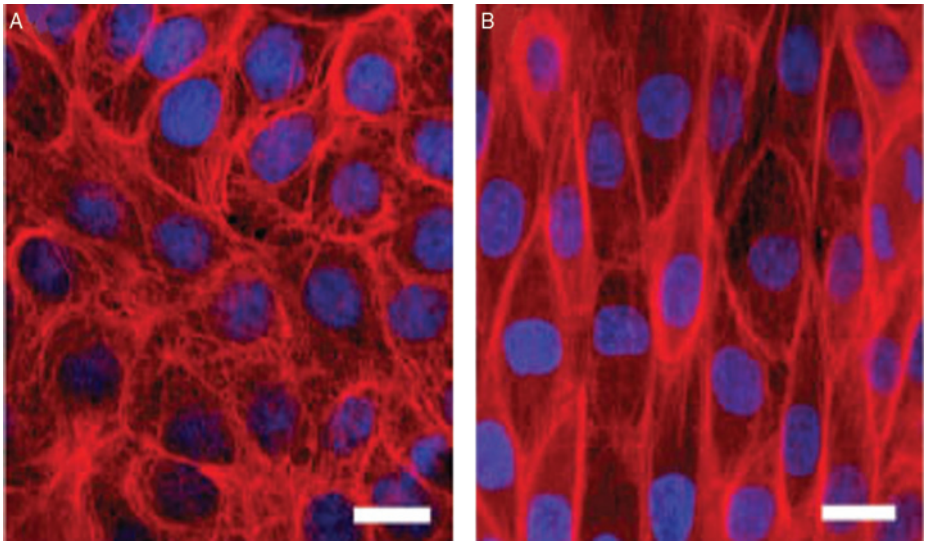

Fig. 14 Effect of stretch on intermediate filament networks in MDCK cells. Control cells (left). Cell after uniaxial stretch (right). Keratins (red) and nuclei (blue) (with permission, Kreplak and Fudge, 2007).

mechanical properties (Herrmann and Aebi, 2004; Kreplak and Fudge, 2007). The assembly of IFs is quite complex and distinct from the assembly process of F-actin or microtubules (Herrmann and Aebi, 1998; Herrmann *et al.*, 1999). The molecular building blocks of IFs are fibrous α-helical proteins that associate laterally and longitudinally to form a bundle of coiled-coils. The diameter of the filament depends on the specific protein, assembly conditions, and may also vary along the length of a single filament. Unlike F-actin or microtubules, these filaments are nonpolar. Moreover, the length of individual filaments and the details of connectivity between filaments in the cytoskeleton are poorly understood. IF assembly is tightly regulated by the cell and can be highly dynamic with turnover rates similar to those for F-actin or microtubules (Helfand *et al.*, 2004).

B. Mechanics of IFs

Recent measurements show that the structure of IFs leads to single filament mechanics that are different from both actin and microtubules (Guzman *et al.*, 2006; Kiss *et al.*, 2006; Kreplak and Fudge, 2007; Kreplak *et al.*, 2005). Imaging measurements suggest that the persistence length for vimentin filaments is on the order of 1 μm, one order of magnitude smaller than for F-actin and three orders of magnitude smaller than for microtubules (Mucke *et al.*, 2004).

Atomic force microscopy measurements of single IFs that are either adsorbed to a solid surface or lying across a small well give us estimates of the single filament extensibility and bending modulus, respectively. Measurements of both unstabilized and glutaraldehyde-stabilized vimentin filaments lying across small wells suggest a bending modulus of 300 MPa and Young's modulus of 900 MPa, but a shear modulus of only 2 MPa (Guzman *et al.*, 2006). This work implies that individual subunits in the filament may slide relative to each other, yielding a complicated bending modulus that actually depends on the type of deformation and the filament length.

Measurements of neurofilaments, desmin, and keratin adsorbed to a solid substrate show that the filaments can be stretched several times their original length before breaking (Kreplak *et al.*, 2005). Stretching of the filament is associated with a marked decrease in the filament diameter, perhaps associated with an irreversible structural transition. The full stress–strain curve for individual IFs is not yet known, but some insight can be drawn from large bundles of IFs that are found in the slime produced by hagfish (Fudge *et al.*, 2003). These IF bundles are highly extensible, like the single filaments, and can support very large stresses before breaking. This impressive extensibility places IFs in stark contrast to actin or microtubules, which break under small extensional strains. These unique mechanical properties suggest a role for IFs in providing mechanical stability to cells that are subjected to large deformations.

C. Mechanics of Networks

Compared to networks of cross-linked actin filaments, the mechanical properties of IF networks have been less widely studied. Here, we describe results from two IF systems. Vimentin networks have a concentration-dependent linear elastic modulus that ranges between 10 and 100 Pa (Janmey *et al.*, 1991). These networks strain stiffen and can withstand large stresses and strains before rupturing, possibly reflecting the extensibility of the individual filaments themselves. The mechanics of neurofilament networks in many ways look similar to the behavior of cross-linked actin networks, with effective cross-linking thought to be provided by interactions between the highly charged sidearms that protrude from the filaments (Rammensee *et al.*, 2007; Fig. 15). These networks show strain-stiffening behavior, but with a different dependence of the modulus on stress than is seen in rigidly cross-linked actin networks. This suggests that the underlying physical mechanism for stiffening in these networks may not be the same type as that discussed in Section II.C.2.

Understanding the physical principles that regulate the dynamics and stress transmission in these complex IF networks remains a current challenge. Furthermore, exploring the mechanical responses of composite networks of IFs with microtubules and F-actin will provide new clues about the complex mechanical response of live cells.

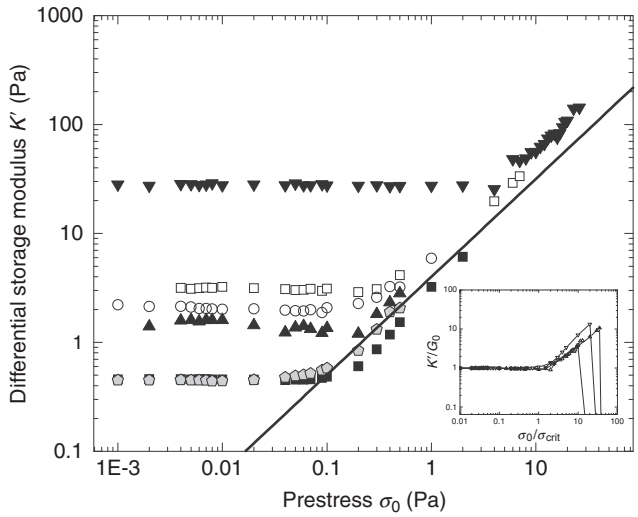

Fig. 15 Nonlinear rheology of neurofilament networks with increasing concentrations: 0.2 mg/ml (filled gray pentagon and filled black square), 0.5 mg/ml (filled up triangle), 0.8 mg/ml (open circle), 1 mg/ml (open square), 5.0 mg/ml (filled upside down triangle). Differential elastic modulus, K', as a function of applied shear prestress. In the nonlinear regime, K' increases nearly linearly with prestress. Inset: Curves from different concentrations can be scaled so that they fall on the same master curve (with permission, Rammensee *et al.*, 2007).

VI. Conclusions and Outlook

Although the importance of understanding cytoskeletal force transmission has been appreciated for some time, recent advances in biochemical and biophysical techniques now enable precise measurements of mechanical response of purified cytoskeletal protein networks over a large range of compositions and length scales. These measurements reveal a wide range of surprising behaviors that arise from the underlying biophysical properties of individual proteins and the nonthermal processes within these networks. In close collaboration with theory, it is now possible to build predictive physical models to describe these behaviors. This process often requires questioning many of the implicit assumptions made when building models of physical, ''nonliving'' materials and is an exciting area of modern materials science. In the context of the cell, it is clear that there is cross talk between all of these cytoskeletal systems. Future work is required to delineate the role of these dynamics and biophysical processes in complex cellular processes such as cell division and migration.

Acknowledgments

MLG would like to acknowledge support from a Career Award at the Scientific Interfaces from the Burroughs Wellcome Fund as well as a NIH Director's Pioneer Award.

References

Bendix, P. M., Koenderink, G. H., Cuvelier, D., Dogic, Z., Koeleman, B. N., Brieher, W. M., Field, C. M., Mahadevan, L., and Weitz, D. A. (2008). A quantitative analysis of contractility in active cytoskeletal protein networks. *Biophys. J.* **94**(8), 3126–3136.

Bicek, A. D., Tuzel, E., Kroll, D. M., and Odde, D. J. (2007). Analysis of microtubule curvature. *Methods Cell Biol.* **83,** 237–268.

Brangwynne, C. P., Koenderink, G. H., Barry, E., Dogic, Z., MacKintosh, F. C., and Weitz, D. A. (2007a). Bending dynamics of fluctuating biopolymers probed by automated high-resolution filament tracking. *Biophys. J.* **93**(1), 346–359.

Brangwynne, C. P., Koenderink, G. H., MacKintosh, F. C., and Weitz, D. A. (2007b). Non-equilibrium microtubule fluctuations in a model cytoskeleton. *Phys. Rev. Lett.* **100**(11), 118104.

Brangwynne, C. P., MacKintosh, F. C., Kumar, S., Geisse, N. A., Talbot, J., Mahadevan, L., Parker, K. K., Ingber, D. E., and Weitz, D. A. (2006). Microtubules can bear enhanced compressive loads in living cells because of lateral reinforcement. *J. Cell Biol.* **173**(5), 733–741.

Brangwynne, C. P., MacKintosh, F. C., and Weitz, D. A. (2007c). Force fluctuations and polymerization dynamics of intracellular microtubules. *Proc. Natl. Acad. Sci. USA* **104**(41), 16128–16133.

Bugyi, B., Papp, G., Hild, G., Lorinczy, D., Nevalainen, E. M., Lappalainen, P., Somogyi, B., and Nyitrai, M. (2006). Formins regulate actin filament flexibility through long range allosteric interactions. *J. Biol. Chem.* **281**(16), 10727–10736.

Bustamante, C., Marko, J. F., Siggia, E. D., and Smith, S. (1994). Entropic elasticity of lambda-phage DNA. *Science* **265**(5178), 1599–1600.

Chaudhuri, O., Parekh, S. H., and Fletcher, D. A. (2007). Reversible stress softening of actin networks. *Nature* **445**(7125), 295–298.

Crocker, J. C., and Hoffman, B. D. (2007). Multiple-particle tracking and two-point microrheology in cells. *Methods Cell Biol.* **83,** 141–178.

Das, M., MacKintosh, F. C., and Levine, A. J. (2007). Effective medium theory of semiflexible filamentous networks. *Phys. Rev. Lett.* **99**(3), 038101.

de Pablo, P., Schaap, I. A. T., MacKintosh, F. C., and Schmidt, C. F. (2003). Deformation and collapse of microtubules on the nanometer scale. *Phys. Rev. Lett.* **91**(9), 098101.

Dogterom, M., and Yurke, B. (1997). Measurement of the force-velocity relation for growing microtubules. *Science* **278,** 856–860.

Fabry, B., Maksym, G. N., Butler, J. P., Glogauer, M., Navajas, D., and Fredberg, J. J. (2001). Scaling the microrheology of living cells. *Phys. Rev. Lett.* **87**(14), 148102.

Felgner, H., Frank, R., and Schliwa, M. (1996). Flexural rigidity of microtubules measured with the use of optical tweezers. *J. Cell Sci.* **109**(Pt 2), 509–516.

Fixman, M., and Kovac, J. (1973). Polymer conformational statistics. III. Modified Gaussian models of stiff chains. *J. Chem. Phys.* **58,** 1564.

Fudge, D. S., Gardner, K. H., Forsyth, V. T., Riekel, C., and Gosline, J. M. (2003). The mechanical properties of hydrated intermediate filaments: Insights from hagfish slime threads. *Biophys. J.* **85**(3), 2015–2027.

Furuike, S., Ito, T., and Yamazaki, M. (2001). Mechanical unfolding of single filamin A (ABP-280) molecules detected by atomic force microscopy. *FEBS Lett.* **498**(1), 72–75.

Gardel, M. L., Nakamura, F., Hartwig, J. H., Crocker, J. C., Stossel, T. P., and Weitz, D. A. (2006a). Stress-dependent elasticity of composite actin networks as a model for cell behavior. *Phys. Rev. Lett.* **96**(8), 088102.

Gardel, M. L., Nakamura, F., Hartwig, J. H., Crocker, J. C., Stossel, T. P., and Weitz, D. A. (2006b). Prestressed F-actin networks cross-linked by hinged filamins replicate mechanical properties of cells. *Proc. Natl. Acad. Sci. USA* **103**(6), 1762–1767.

Gardel, M. L., Shin, J. H., MacKintosh, F. C., Mahadevan, L., Matsudaira, P. A., and Weitz, D. A. (2004a). Elastic behavior of cross-linked and bundled actin networks. *Science* **304**(5675), 1301–1305.

Gardel, M. L., Shin, J. H., MacKintosh, F. C., Mahadevan, L., Matsudaira, P. A., and Weitz, D. A. (2004b). Scaling of F-actin network rheology to probe single filament elasticity and dynamics. *Phys. Rev. Lett.* **93**(18), 188102.

Gardel, M. L., Valentine, M. T., Crocker, J. C., Bausch, A. R., and Weitz, D. A. (2003). Microrheology of entangled F-actin solutions. *Phys. Rev. Lett.* **91**(15), 158302.

Gittes, F., Mickey, B., Nettleton, J., and Howard, J. (1993). Flexural rigidity of microtubules and actin filaments measured from thermal fluctuations in shape. *J. Cell Biol.* **120**(4), 923–934.

Guzman, C., Jeney, S., Kreplak, L., Kasas, S., Kulik, A. J., Aebi, U., and Forro, L. (2006). Exploring the mechanical properties of single vimentin intermediate filaments by atomic force microscopy. *J. Mol. Biol.* **360**(3), 623–630.

Head, D. A., Levine, A. J., and MacKintosh, F. C. (2003a). Deformation of cross-linked semiflexible polymer networks. *Phys. Rev. Lett.* **91**(10), 108102.

Head, D. A., Levine, A. J., and MacKintosh, F. C. (2003b). Distinct regimes of elastic response and deformation modes of cross-linked cytoskeletal and semiflexible polymer networks. *Phys. Rev. E Stat. Nonlin. Soft. Matter Phys.* **68**(6 Pt 1), 061907.

Helfand, B. T., Chang, L., and Goldman, R. D. (2004). Intermediate filaments are dynamic and motile elements of cellular architecture. *J. Cell Sci.* **117**(Pt 2), 133–141.

Herrmann, H., and Aebi, U. (1998). Intermediate filament assembly: Fibrillogenesis is driven by decisive dimer-dimer interactions. *Curr. Opin. Struct. Biol.* **8**(2), 177–185.

Herrmann, H., and Aebi, U. (2004). Intermediate filaments: Molecular structure, assembly mechanism, and integration into functionally distinct intracellular Scaffolds. *Annu. Rev. Biochem.* **73,** 749–789.

Herrmann, H., Haner, M., Brettel, M., Ku, N. O., and Aebi, U. (1999). Characterization of distinct early assembly units of different intermediate filament proteins. *J. Mol. Biol.* **286**(5), 1403–1420.

Humphrey, D., Duggan, C., Saha, D., Smith, D., and Kas, J. (2002). Active fluidization of polymer networks through molecular motors. *Nature* **416**(6879), 413–416.

Ingber, D. E. (1997). Tensegrity: The architectural basis of cellular mechanotransduction. *Annu. Rev. Physiol.* **59,** 575–599.

Ingber, D. E. (2003). Tensegrity I. Cell structure and hierarchical systems biology. *J. Cell Sci.* **116**(7), 1157–1173.

Isambert, H., Venier, P., Maggs, A. C., Fattoum, A., Kassab, R., Pantaloni, D., and Carlier, M. F. (1995). Flexibility of actin filaments derived from thermal fluctuations. Effect of bound nucleotide, phalloidin, and muscle regulatory proteins. *J. Biol. Chem.* **270**(19), 11437–11444.

Janmey, P. A., Euteneuer, U., Traub, P., and Schliwa, M. (1991). Viscoelastic properties of vimentin compared with other filamentous biopolymer networks. *J. Cell Biol.* **113**(1), 155–160.

Janmey, P. A., McCormick, M. E., Rammensee, S., Leight, J. L., Georges, P. C., and MacKintosh, F. C. (2007). Negative normal stress in semiflexible biopolymer gels. *Nat. Mater.* **6**(1), 48–51.

Janson, M. E., and Dogterom, M. (2004). A bending mode analysis for growing microtubules: Evidence for a velocity-dependent rigidity. *Biophys. J.* **87,** 2723–2736.

Kas, J., Strey, H., and Sackmann, E. (1993). Direct measurement of the wave-vector-dependent bending stiffness of freely flickering actin filaments. *Europhys. Lett.* **21,** 865–870.

Kasza, K. E., Rowat, A. C., Liu, J., Angelini, T. E., Brangwynne, C. P., Koenderink, G. H., and Weitz, D. A. (2007). The cell as a material. *Curr. Opin. Cell Biol.* **19**(1), 101–107.

Kikumoto, M., Kurachi, M., Tosa, V., and Tashiro, H. (2006). Flexural rigidity of individual microtubules measured by a buckling force with optical traps. *Biophys. J.* **90,** 1687–1696.

Kirschner, M., and Mitchison, T. (1986). Beyond self-assembly: From microtubules to morphogenesis. *Cell* **45**(3), 329–342.

Kiss, B., Karsai, A., and Kellermayer, M. S. (2006). Nanomechanical properties of desmin intermediate filaments. *J. Struct. Biol.* **155**(2), 327–339.

Koenderink, G. H., Atakhorrami, M., MacKintosh, F. C., and Schmidt, C. F. (2006). High-frequency stress relaxation in semiflexible polymer solutions and networks. *Phys. Rev. lett.* **96,** 138307.

Kojima, H., Ishijima, A., and Yanagida, T. (1994). Direct measurement of stiffness of single actin filaments with and without tropomyosin by *in vitro* nanomanipulation. *Proc. Natl. Acad. Sci. USA* **91** (26), 12962–12966.

Kowalski, R. J., and Williams, R. C., Jr. (1993). Microtubule-associated protein 2 alters the dynamic properties of microtubule assembly and disassembly. *J. Biol. Chem.* **268**(13), 9847–9855.

Kreis, T., and Vale, R. (1999). ''Guidebook to the Cytoskeletal and Motor Proteins.'' Oxford University Press, New York.

Kreplak, L., Bar, H., Leterrier, J. F., Herrmann, H., and Aebi, U. (2005). Exploring the mechanical behavior of single intermediate filaments. *J. Mol. Biol.* **354**(3), 569–577.

Kreplak, L., and Fudge, D. (2007). Biomechanical properties of intermediate filaments: From tissues to single filaments and back. *Bioessays* **29**(1), 26–35.

Lieleg, O., and Bausch, A. R. (2007). Cross-linker unbinding and self-similarity in bundled cytoskeletal networks. *Phys. Rev. Lett.* **99,** 158105.

Lin, Y. C., Koenderink, G. H., MacKintosh, F. C., and Weitz, D. A. (2007). Viscoelastic properties of microtubule networks. *Macromolecules* **40,** 7714–7720.

Liu, J., Gardel, M. L., Kroy, K., Frey, E., Hoffman, B. D., Crocker, J. C., Bausch, A. R., and Weitz, D. A. (2006). Microrheology probes length scale dependent rheology. *Phys. Rev. Lett.* **96** (11), 118104.

Liu, J., Koenderink, G. H., Kasza, K. E., Mackintosh, F. C., and Weitz, D. A. (2007). Visualizing the strain field in semiflexible polymer networks: Strain fluctuations and nonlinear rheology of F-actin gels. *Phys. Rev. Lett.* **98**(19), 198304.

Liu, X., and Pollack, G. H. (2002). Mechanics of F-actin characterized with microfabricated cantilevers. *Biophys. J.* **83**(5), 2705–2715.

Lodish, H., Berk, A., Zipursky, S. L., Matsudaira, P., Baltimore, D., and Darnell, D. (1999). ''Molecular Cell Biology.'' W.H. Freeman Co., New York.

MacKintosh, F. C., Kas, J., and Janmey, P. A. (1995). Elasticity of semiflexible biopolymer networks. *Phys. Rev. Lett.* **75**(24), 4425–4428.

Mitchison, T., and Kirschner, M. (1984). Dynamic instability of microtubule growth. *Nature* **312**(15), 237–242.

Mizuno, D., Tardin, C., Schmidt, C. F., and Mackintosh, F. C. (2007). Nonequilibrium mechanics of active cytoskeletal networks. *Science* **315**(5810), 370–373.

Mucke, N., Kreplak, L., Kirmse, R., Wedig, T., Herrmann, H., Aebi, U., and Langowski, J. (2004). Assessing the flexibility of intermediate filaments by atomic force microscopy. *J. Mol. Biol.* **335**(5), 1241–1250.

Needleman, D. J., Ojeda-Lopez, M. A., Raviv, U., Ewert, K., Jones, J. B., Miller, H. P., Wilson, L., and Safinya, C. R. (2004). Synchrotron X-ray diffraction study of microtubules buckling and bundling under osmotic stress: A probe of interprotofilament interactions. *Phys. Rev. Lett.* **93**(19), 198104.

Ott, A., Magnasco, M., Simon, A., and Libchaber, A. (1993). Measurement of the persistence length of polymerized actin using fluorescence microscopy. *Phys. Rev. E Stat. Phys. Plasmas Fluids Relat. Interdiscip. Topics* **48**(3), R1642–R1645.

Paluch, E., van der Gucht, J., and Sykes, C. (2006). Cracking up: Symmetry breaking in cellular systems. *J. Cell Biol.* **175**(5), 687–692.

Pampaloni, F., Lattanzi, G., Jonas, A., Surrey, T., Frey, E., and Florin, E. L. (2006). Thermal fluctuations of grafted microtubules provide evidence of a length-dependent persistence length. *Proc. Natl. Acad. Sci. USA* **103**(27), 10248–10253.

Panorchan, P., Lee, J. S., Daniels, B. R., Kole, T. P., Tseng, Y., and Wirtz, D. (2007). Probing cellular mechanical responses to stimuli using ballistic intracellular nanorheology. *Methods Cell Biol.* **83,** 115–140.

Poirier, M. G., and Marko, J. F. (2002). Effect of internal friction on biofilament dynamics. *Phys. Rev. Lett.* **88**(22), 228103.

Radmacher, M. (2007). Studying the mechanics of cellular processes by atomic force microscopy. *Methods Cell Biol.* **83,** 347–372.

Rammensee, S., Janmey, P. A., and Bausch, A. R. (2007). Mechanical and structural properties of *in vitro* neurofilament hydrogels. *Eur. Biophys. J.* **36**(6), 661–668.

Sato, M., Schwarz, W. H., and Pollard, T. D. (1987). Dependence of the mechanical properties of actin/alpha-actinin gels on deformation rate. *Nature* **325**(6107), 828–830.

Schulze, E., and Kirschner, M. (1986). Microtubule dynamics in interphase cells. *J. Cell Biol.* **102**(3), 1020–1031.

Shin, J. H., Gardel, M. L., Mahadevan, L., Matsudaira, P., and Weitz, D. A. (2004). Relating microstructure to rheology of a bundled and cross-linked F-actin network *in vitro*. *Proc. Natl. Acad. Sci. USA* **101**(26), 9636–9641.

Smith, D. M., Ziebert, F., Humphrey, D., Duggan, C., Steinbeck, M., Zimmermann, W., and Kas, J. A. (2007). Molecular motor-induced instabilities and crosslinkers determine biopolymer organization. *Biophys. J.* **93**(12), 4445–4452.

Storm, C., Pastore, J. J., MacKintosh, F. C., Lubensky, T. C., and Janmey, P. A. (2005). Nonlinear elasticity in biological gels. *Nature* **435**(7039), 191–194.

Stossel, T. P., Condeelis, J., Cooley, L., Hartwig, J. H., Noegel, A., Schleicher, M., and Shapiro, S. S. (2001). Filamins as integrators of cell mechanics and signalling. *Nat. Rev. Mol. Cell Biol.* **2**(2), 138–145.

Tempel, M., Isenberg, G., and Sackmann, E. (1996). Temperature-induced sol-gel transition and microgel formation in alpha-actinin cross-linked actin networks: A rheological study. *Phys. Rev. E Stat. Phys. Plasmas Fluids Relat. Interdiscip. Topics* **54**(2), 1802–1810.

Valentine, M. T., Perlman, Z. E., Gardel, M. L., Shin, J. H., Matsudaira, P., Mitchison, T. J., and Weitz, D. A. (2004). Colloid surface chemistry critically affects multiple particle tracking measurements of biomaterials. *Biophys. J.* **86**(6), 4004–4014.

Venier, P., Maggs, A. C., Carlier, M. F., and Pantaloni, D. (1994). Analysis of microtubule rigidity using hydrodynamic flow and thermal fluctuations. *J. Biol. Chem.* **269**(18), 13353–13360.

Visegrady, B., Lorinczy, D., Hild, G., Somogyi, B., and Nyitrai, M. (2004). The effect of phalloidin and jasplakinolide on the flexibility and thermal stability of actin filaments. *FEBS Lett.* **565**(1–3), 163–166.

Wachsstock, D. H., Schwartz, W. H., and Pollard, T. D. (1993). Affinity of alpha-actinin for actin determines the structure and mechanical properties of actin filament gels. *Biophys. J.* **65**(1), 205–214.

Wagner, B., Tharmann, R., Haase, I., Fischer, M., and Bausch, A. R. (2006). Cytoskeletal polymer networks: The molecular structure of cross-linkers determines macroscopic properties. *Proc. Natl. Acad. Sci. USA* **103**(38), 13974–13978.

Waterman-Storer, C. M., and Salmon, E. D. (1997). Actomyosin-based retrograde flow of microtubules in the lamella of migrating epithelial cells influences microtubule dynamic instability and turnover and is associated with microtubule breakage and treadmilling. *J. Cell Biol.* **139**(2), 417–434.

Weihs, D., Mason, T. G., and Teitell, M. A. (2006). Bio-microrheology: A frontier in microrheology. *Biophys. J.* **91**(11), 4296–4305.

Weins, A., Kenlan, P., Herbert, S., Le, T. C., Villegas, I., Kaplan, B. S., Appel, G. B., and Pollak, M. R. (2005). Mutational and biological analysis of alpha-actinin-4 in focal segmental glomerulosclerosis. *J. Am. Soc. Nephrol.* **16**(12), 3694–3701.

Wong, I. Y., Gardel, M. L., Reichman, D. R., Weeks, E. R., Valentine, M. T., Bausch, A. R., and Weitz, D. A. (2004). Anomalous diffusion probes microstructure dynamics of entangled F-actin networks. *Phys. Rev. Lett.* **92**(17), 178101.

Xu, J., Tseng, Y., and Wirtz, D. (2000). Strain hardening of actin filament networks. Regulation by the dynamic cross-linking protein alpha-actinin. *J. Biol. Chem.* **275**(46), 35886–35892.

Xu, J., Wirtz, D., and Pollard, T. D. (1998). Dynamic cross-linking by alpha-actinin determines the mechanical properties of actin filament networks. *J. Biol. Chem.* **273**(16), 9570–9576.

Yao, J., Le, T. C., Kos, C. H., Henderson, J. M., Allen, P. G., Denker, B. M., and Pollak, M. R. (2004). Alpha-actinin-4-mediated FSGS: An inherited kidney disease caused by an aggregated and rapidly degraded cytoskeletal protein. *PLoS Biol.* **2**(6), e167.